Eur. Phys. J. D **39**, 423–432 (2006)
DOI: 10.1140/epjd/e2006-00118-y

THE EUROPEAN PHYSICAL JOURNAL D

Hyperthermal cluster-surface scattering

Comparison of fragmentation, energy redistribution, and sticking in atomic and molecular clusters

S. Zimmermann and H.M. Urbassek[a]

Fachbereich Physik, Universität Kaiserslautern, Erwin-Schrödinger-Straße, 67663 Kaiserslautern, Germany

Received 31 January 2006 / Received in final form 27 March 2006
Published online 7 June 2006 –

Abstract. Using molecular-dynamics simulation, we study the processes occurring after impact of clusters on a rigid wall. Comparing the impact of model clusters consisting of 13 atoms, or of 13 diatomic molecules with varied bond strength, the systematics in the results of the collision process are investigated. Four regimes of impact-induced cluster fragmentation are identified: intact reflection, shattering into large fragments, complete fragmentation, and molecule dissociation. The effect of the number of degrees of freedom activated in the collision on the translational and internal energies of the reflected fragments is discussed in detail. As a rule, with increasing number of degrees of freedom which can be activated in the collision, the translational energy sinks. On the other hand, for weak intramolecular bonding, intramolecular vibrations are easily excited at small impact energies, reducing the resulting translational energy. The presence of even a very weak attractive well ϵ_w at the surface has a major influence on the sticking behavior of the clusters — and hence also on the absolute reflected energies — even at impact energies $E_0 \gg \epsilon_w$.

PACS. 68.49.Fg Cluster scattering from surfaces – 36.40.-c Atomic and molecular clusters – 79.20.Ap Theory of impact phenomena; numerical simulation

1 Introduction

The interaction of hyperthermal clusters impinging on solid surfaces has received increased attention in the recent past. From a fundamental point of view, processes such as the short-time extreme local densities, pressures and kinetic temperatures reached [1] or the induced electronic excitations [2] were investigated. From an applied point of view, controlled cluster deposition [3] (soft landing) [4] or surface cleaning by cluster impact [5] give promising prospects. In the field of cluster-impact chemistry, a number of intriguing experiments on the cluster fragmentation, the collisional energy loss, collision-induced dissociation and even impact-induced chemical reactions have been performed and accompanied by molecular-dynamics simulations [6].

The field of thermal and also hyperthermal *atom*-surface collisions has been well covered in the past and reached a mature understanding [7,8]. Here, the properties of the reflected atoms can be parameterized in terms of the atom energy (or gas temperature), the surface temperature, the mass ratio of projectile and surface atoms, and the depth of the attractive well. From the theoretical point of view, quite early the so-called soft- and hard-cube models have been developed to describe these collisions [7,9,10]. While the field of thermal atom- and molecule-surface interaction have been investigated quite thoroughly in the past decades, the experimental and theoretical progress in the hyperthermal velocity regime has not yet reached comparable maturity [11].

If a *cluster* collides with a surface, besides the parameters mentioned above, a considerable number of further parameters enter, such as the number of cluster atoms, the intermolecular bonding in the cluster, and also the intramolecular bonding in case the cluster consists of molecular constituents. Hence it appears impossible to perform a systematic study of the generic aspects of cluster-surface interaction, such as it is possible in hyperthermal atom-surface scattering. Thus, many existing simulational studies of cluster-surface interaction modelled concrete specific cases, often in combination with experiments performed in the same group [12–14].

Computer simulations of cluster-surface interaction have been performed repeatedly in the past. Simulations [1,14–19] of the impact of rare-gas clusters on surfaces have demonstrated the extensive or even complete fragmentation of the impinging cluster occurring at higher impact velocities. Also, simulations of specific molecular clusters such as $(NH_3)_nH^+$ and also of mixed species such as I_2Ar_n and $(CH_3I)_n^-$ have been performed [19–21]. In these studies, as a rule only the rotational degrees of

[a] e-mail: urbassek@rhrk.uni-kl.de

freedom of the molecules were included. In another interesting study [14], Christen et al. showed in a combined experimental and simulational approach that at low cluster velocities a regime of 'deep inelastic scattering' occurs where the clusters lose most of their initial kinetic energy upon scattering off the surface. In earlier papers [18, 22], Raz et al. used a maximum-entropy argument to show that the transition from (low-energy) evaporation of a few atoms to (high-energy) shattering into many fragments shows a rather sharp transition as a function of the impact energy. This transition was termed 'shattering transition' and occurs when the cluster energy per atom exceeds the bond energy, or in other words, the cluster temperature exceeds the 'boiling temperature'.

In the present paper, we wish to employ molecular-dynamics simulation to shed light on systematic effects of cluster-surface interaction such as the fragmentation, the sticking, and the energy redistribution channels after reflection. In particular, we want to investigate the basic issue in how far the scattering of a molecular cluster differs from that of an atomic cluster. We wish to shed light on this question by exploring an idealized but exemplary model situation. While modelling a specific case, viz. the collision of a 13-molecule cluster off a rigid wall, we want to answer a general question, i.e., in how far the intramolecular degrees of freedom are important in determining the outcome of the collision. We shall answer this question by comparing the collision of three clusters with a wall: an atomic cluster, a strongly-bonded molecular cluster, and a weakly-bonded molecular cluster, and show that indeed the molecular or atomic nature of the cluster leads to sensitive changes in the distribution of the cluster fragments, such as for example the translational energy.

2 System

2.1 Clusters

In this study, we wish to compare the reflection of various icosahedral clusters, containing 13 atoms or molecules, from a rigid wall. Three different clusters are employed:

1. a molecular cluster, consisting of 13 N_2 molecules. The intramolecular bonding has been chosen as a Morse potential,

$$V_{\text{intra}}(r) = D\left[e^{-2(r-r_0)/\lambda} - 2e^{-(r-r_0)/\lambda}\right], \quad (1)$$

with parameters $D = 9.99$ eV, $r_0 = 1.0977$ Å, and $\lambda = 0.2696$ Å; the mass of an N atom is $m = 14$ amu [23,24]. This bond is so stiff that vibrational excitation is negligible; the bond can be considered rigid. The intermolecular interaction potential, acting between atoms belonging to different molecules only, is chosen as an atomic pairwise Lennard-Jones potential

$$V_{\text{inter}}(r) = 4\epsilon\left[\left(\frac{\sigma}{r}\right)^{12} - \left(\frac{\sigma}{r}\right)^{6}\right] \quad (2)$$

with parameters $\epsilon = 3.212$ meV and $\sigma = 3.31$ Å [25,26]. The total intermolecular binding energy of the cold cluster will be denoted by Φ and amounts to

$$\Phi = 439 \text{ meV}; \quad (3)$$

2. an atomic cluster, denoted by A_{13}, with a Lennard-Jones interatomic interaction potential, equation (2), with the same value of the length scale σ, but an increased energy scale $\epsilon_A = 3.09\epsilon$, which was chosen such as to obtain the same binding energy for the ground state 13-atom cluster, Φ, as the intermolecular energy of the N_2 cluster, equation (3). Also, the mass of this atom has been chosen twice the mass of a nitrogen atom, $M_A = 2m$;
3. since N_2 molecules are very stiff, we also studied a hypothetical reference cluster, in which the intramolecular bonding D was softened by a factor 100, while all other parameters of the inter- and intramolecular bonding have been kept unchanged. This cluster will be denoted in the following as $(\psi_2)_{13}$. We made sure that this cluster has the same ground-state geometry as the N_2 cluster and hence the same ground-state energy Φ, equation (3).

In choosing these energy parameters, we are able to obtain a clear distinction in energy scales between the intermolecular bond (3 meV), the weak intramolecular bond (100 meV) and the strong intramolecular bond (10 eV). All potentials have been cut off at $r_{\text{cut}} = 3.5\sigma = 11.585$ Å. The ground state of the atomic cluster is an icosahedron [27], cf. Figure 1a. The corresponding molecular clusters are shown in Figure 1b. The centers of mass of the molecules are again organized as an icosahedron, but the molecular orientations had to be found by an energy minimization routine.

2.2 Wall

The rigid, uncorrugated wall considered in this study is modelled by an external potential, which acts on each cluster atom and depends only on the perpendicular distance z of the atom to the wall. We study both a purely repulsive potential,

$$V_{\text{wall}}^{\text{rep}}(z) = \begin{cases} 4\epsilon_w\left[\left(\frac{\sigma_w}{z}\right)^{12} - \left(\frac{\sigma_w}{z}\right)^{6}\right] + \epsilon_w, & z < 2^{1/6}\sigma_w \\ 0, & z \geq 2^{1/6}\sigma_w, \end{cases} \quad (4)$$

and a weakly attractive potential,

$$V_{\text{wall}}^{\text{attr}}(z) = 4\epsilon_w\left[\left(\frac{\sigma_w}{z}\right)^{12} - \left(\frac{\sigma_w}{z}\right)^{6}\right]. \quad (5)$$

The potential parameters ϵ_w and σ_w are chosen to have the same values as for the intermolecular interaction of the N_2-molecules, equation (2).

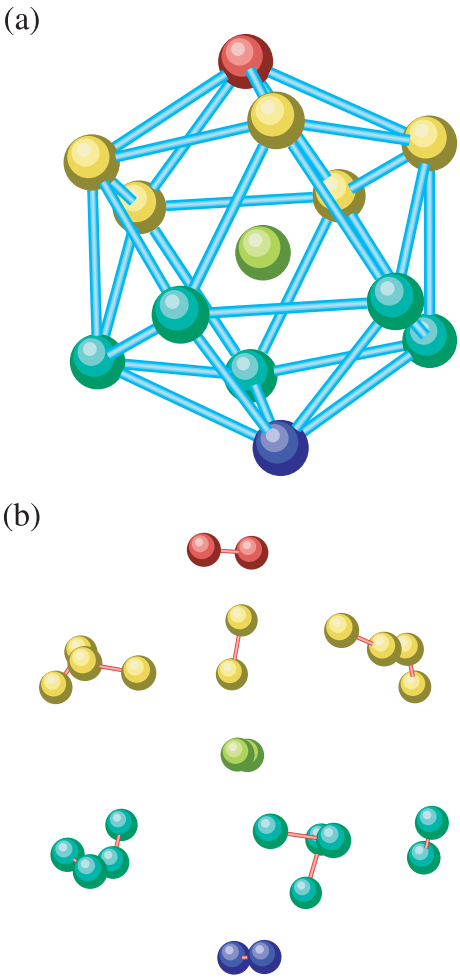

Fig. 1. (Color online) Perspective view of the atomic (a) and the molecular (b) cluster. Several of the interatomic bonds are indicated in (a) to help visualize the structure; these are omitted in (b), where only the intramolecular bonds are plotted in red. The color of the atoms helps to visualize the three-dimensional structure of the clusters.

2.3 Simulation

The molecular-dynamics code is standard [28]. It employs the velocity Verlet integrator to solve Newtons's equations of motion. In order to resolve the vibrational motion in the molecular systems, the time step is chosen rather small, 0.1 fs.

In the simulation, the cluster is initially positioned at a distance $z > r_{\rm cut}$ in front of the wall such that the cluster has no interaction with it. The cluster is at temperature zero, it does not vibrate or rotate. Each simulation has been performed with two cluster orientations: (i) with an atom/molecule pointing towards the surface (tip geometry), and (ii) with a cluster face pointing towards the surface (face geometry). Since the differences in the results of these two orientations are only minor, in the following only the averages over these two orientations will be discussed.

The cluster is given a kinetic center-of-mass energy E_0 with a momentum directed perpendicular to the surface. We study energies E_0 ranging from 1 meV to 20 eV; the corresponding center-of-mass velocities of the clusters are between 23 m/s and 3.3 km/s. The simulation proceeds until the cluster has been totally reflected from the surface, i.e., until all cluster atoms are again outside the interaction potential with the wall. Depending on E_0, this may take a time between 5 and 100 ps. In the case of an attractive wall, fragments may remain adsorbed in the attractive potential well; also in this case, we terminate the simulation after 100 ps at most.

As a consequence of the interaction of the cluster with the wall, the cluster may break up. We shall denote as 'fragmentation' the process where the cluster dissolves into its (molecular) constituents, and as 'dissociation' the breaking of the intramolecular bond. In the case of the atomic cluster A_{13}, only fragmentation, but no dissociation can occur; in the case of the $(N_2)_{13}$-cluster no dissociation was observed.

3 Results: reflection from a repulsive wall

3.1 Fragmentation

After reflection, we identify the cluster fragments using a cluster-detection algorithm [29]. This algorithm subdivides all atoms into disjoint sets; the atoms in any such set have zero interaction energy with the atoms of the other sets, but non-zero interaction with at least one other atom of the same set. We identify these disjoint sets with the cluster fragments produced by the collision with the wall.

At each bombarding energy, a different fragment distribution results from the collision. Figures 2a–2d show several characteristics of this distribution: the number of fragments produced, $N_{\rm fr}$, the average fragment size, $\langle m \rangle$, the size of the largest fragment, $m_{\rm max}$, and the number of monomers produced, $N_{\rm mono}$. The latter quantity is shown for an enlarged energy range in Figure 2e. In Figure 2f, we additionally show the number of dissociated molecules; this is relevant only for the case of $(\psi_2)_{13}$, since for the other clusters, no dissociation occurs.

Figure 2a shows that to a first approximation, quite irrespective of the internal structure of the cluster constituents — atoms or weakly- or strongly-bonded molecules —, the average number of fragments produced, $N_{\rm fr}$, increases in a very analogous way as a function of projectile energy. This shows that it is basically the intermolecular bond energy which governs fragmentation. Note that at higher projectile energies, $E_0 \gtrsim 1$ eV, the atomic cluster appears to be more stable than the molecular cluster.

An inspection of the various characteristics of the fragmentation patterns shown in Figures 2a–2f may be summarized as follows: Four regimes of fragmentation patterns can be found for all three cluster types studied here:

(i) for small impact energies $E_0 < 0.2$ eV, the cluster is reflected intact. Interestingly, for molecular clusters, this regime is extended towards larger impact energies; this is due to the fact that the intramolecular bond gives

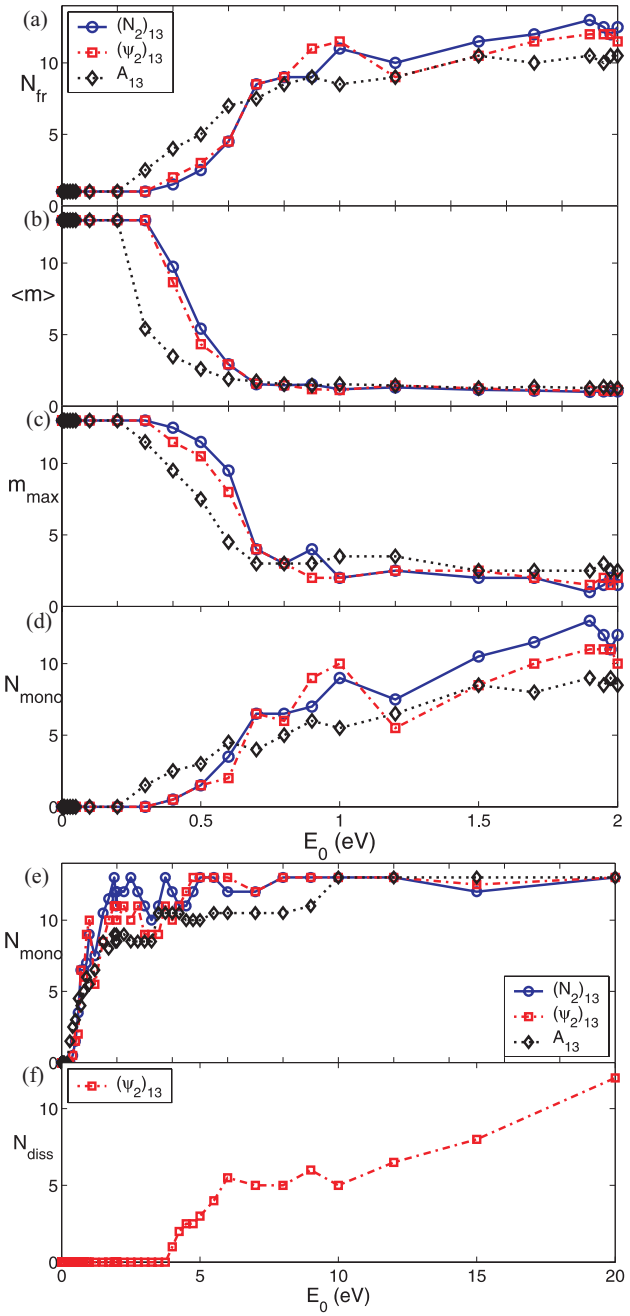

Fig. 2. (Color online) Fragmentation behavior of the cluster after collision with a repulsive wall: (a) average number of fragments, $N_{\rm fr}$, (b) average fragment size, $\langle m \rangle$, (c) size of the largest fragment, $m_{\rm max}$, (d) and (e) average number of monomers, $N_{\rm mono}$, (f) average number of dissociated molecules, $N_{\rm diss}$ [only shown for $(\psi_2)_{13}$].

rise to additional degrees of freedom — in particular frustrated rotations — which are able to store an additional amount of energy, analogous to the increased heat capacity of molecules with respect to atoms;

(ii) partial fragmentation, in which the cluster is decomposed into a number of daughter fragments:
   (a) large fragments and only very few monomers are seen in an energy regime which extends from 0.3 eV up to 0.6 eV for N_2; this regime corresponds to the evaporation of a few monomers off the major remaining daughter fragment cluster,
   (b) a long regime of continuously increasing fragment numbers ensues; this regime has occasionally be called cluster *shattering*. Note that still dimers or occasionally a trimer survive as the largest constituent among the fragments;

(iii) complete fragmentation into individual monomers. Interestingly, this regime starts earlier for molecular clusters (5 eV) than for the atomic cluster (10 eV). Evidently, the energy stored in the intramolecular degrees of freedom now has a detrimental effect on the cluster fragment stability; note that the intermolecular bond is only 3 meV, which is easily overcome by (frustrated) rotational excitation of the molecular constituents of a dimer or trimer;

(iv) full molecular dissociation is only observed for the ψ_2 cluster with its intramolecular bond strength of 100 meV. Figure 2f shows that molecule dissociation starts at around 4 eV; as noted above, at 20 eV all molecules have been destroyed.

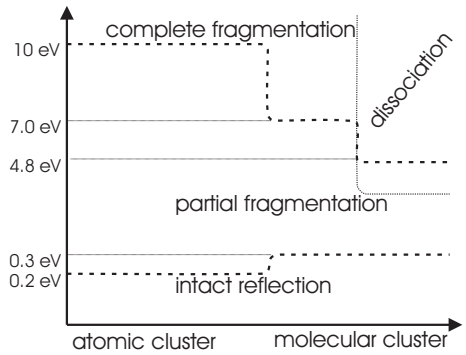

Fig. 3. Schematics of fragmentation regimes in cluster-surface scattering.

Figure 3 gives a schematic overview over the fragmentation regimes observed. We note that, while the existence of several of the regimes discussed — such as in particular that of intact reflection (also known as 'deep inelastic regime') — has been known before [14], the dependence of the regimes on the internal degrees of freedom available in the cluster is novel.

The order of magnitude of the energies necessary for breaking the inter- and intramolecular bonds, respectively, can be estimated via an adiabaticity argument [30]. Vibrations are not excited, and hence bonds are not broken, if the collision time $t_c = \sigma_w/v$ is larger than the vibration period $T = 2\pi/\omega$. Here $v = \sqrt{E_0/13m}$ is the translational velocity of the cluster, and σ_w is the length scale of the wall potential. For the Morse potential, the vibrational frequency is $\omega = (2/\lambda)\sqrt{D/m}$ and hence intramolecular vibrations are only excited when $E_0 \geq 2000$ eV (20 eV) for the N_2 (ψ_2) cluster; for the Lennard-Jones potential, it is $\omega = 12 \times 2^{-1/6}\sqrt{\epsilon/m\sigma^2}$, and hence impact energies $E_0 > 120$ meV are needed to excite intermolecular

vibrations. These numbers are all in the correct order of magnitude for the thresholds depicted in Figures 2 and 3.

Our results of the fragmentation behavior of clusters colliding with a repulsive wall can hence be summarized to indicate that the existence of intramolecular degrees of freedom narrows the regime of partial fragmentation and favors that of intact reflection and complete fragmentation.

3.2 Energy redistribution: atomic cluster

After collision from a repulsive wall, the total impact energy E_0 is found again in the ensemble of cluster fragments reflected off the wall, and the assignment of the energy channels is relatively straightforward, in particular for the atomic cluster. Here, the impact energy can be used for cluster fragmentation, internal fragment excitation, and in the translational energy of clusters moving away from the surface. We proceed as follows.

Let us call $N_{\rm fr}$ the number of fragments produced. For each fragment κ, we calculate the center-of-mass energy $E_{{\rm cm},\kappa}$ and call

$$E_{\rm trans} = \sum_{\kappa=1}^{N_{\rm fr}} E_{{\rm cm},\kappa} \tag{6}$$

the translational energy. Note that these center-of-mass energies $E_{{\rm cm},\kappa}$ are observable in experiment by time-of-flight techniques.

In accordance with the potentials, equations (1) and (2), which fulfill $V(r \to \infty) = 0$, all potential energies given below refer to the reference state of a completely fragmented cluster. We shall call

$$E_{\rm int}^{\rm pot} = \sum_{i<j} V_{\rm inter}(r_{ij}) + \Phi \tag{7}$$

the increase in potential energy due to (partial) fragmentation of the parent cluster and internal excitation of the fragments.

For the atomic cluster, we employ the summed internal kinetic energy of the fragments, $E_{\rm int}^{\rm kin}$, as a measure for the internal fragment excitation ('temperature'), while the fragment potential energy, $E_{\rm int}^{\rm pot}$, as introduced above includes both the energy spent in fragmentation and the internal potential energies. We have the energy balance

$$E_0 = E_{\rm trans} + E_{\rm int}^{\rm kin} + E_{\rm int}^{\rm pot}, \tag{8}$$

which is shown in Figure 4 both as absolute energies and relative to the impact energy E_0.

As discussed above, for $E_0 \gtrsim 0.5$ eV, an almost fixed part of the impact energy is used for cluster break-up. Accordingly, beyond this energy, no cluster excitation occurs. For $E_0 \to 0$, the cluster is reflected elastically from the wall, and all bombarding energy is transferred to the translational energy of the reflected cluster; this corresponds to the adiabatic limit discussed above. With increasing impact energy in the regime of intact reflection,

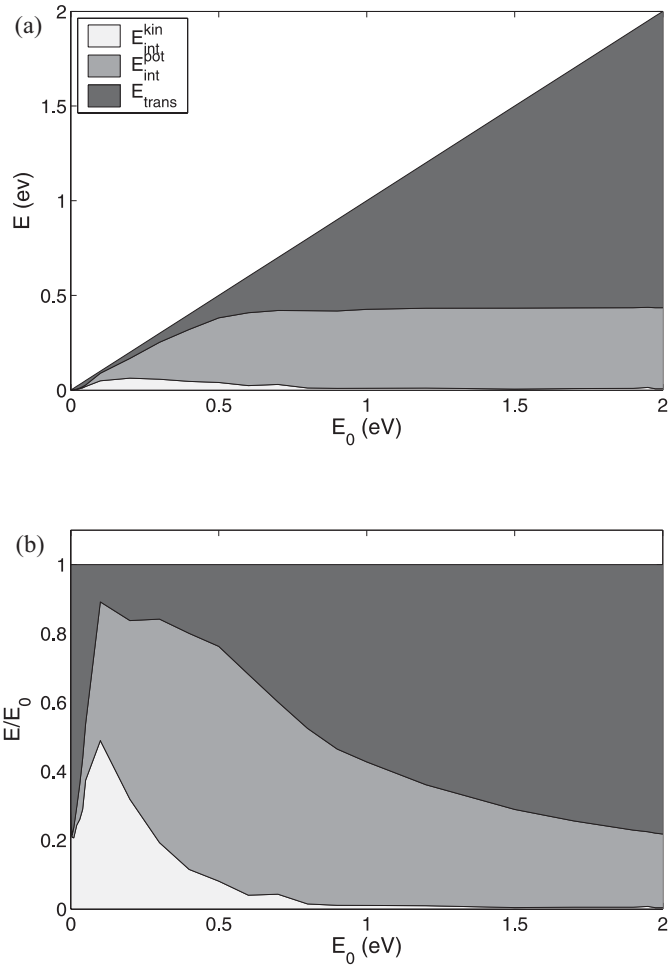

Fig. 4. Energy redistribution in an A_{13} cluster after reflection from a repulsive wall; (a) absolute energies E, (b) energies relative to impact energy E_0.

the relative contribution of the translational energy gradually decreases in favor of the excitation of the internal degrees of freedom of the reflected cluster. Internal kinetic and potential energy are equally populated. This trend is reversed in the partial fragmentation regime, where now an ever larger contribution is given to the translational energy. Concomitantly with the decline of larger clusters in the fragment distribution (cf. Fig. 2c), i.e., in the regime of small fragments, the internal kinetic energy becomes vanishingly small. The constant remainder of the internal potential energy is due to cluster break-up and assumes a fixed value Φ for large E_0. Thus, we conclude that the regimes found in the fragmentation behavior are well reflected in the energy redistribution pattern of atomic clusters.

3.3 Energy redistribution: molecular cluster

If a molecular cluster has been completely fragmented and also totally dissociated to its atomic constituents, the energy $13D$ has been dispensed in breaking the intramolecular bonds, and Φ to fragment the cluster; hence it is

$E_{\rm trans} = E_0 - \Phi - 13D$. However, if molecules or clusters survived the reflection process, further internal (potential and kinetic) energy forms are present. Due to the possibility of inter- and intramolecular energy couplings, their analysis is not so straightforward. We will proceed as follows:

1. for the *strongly-bound* molecular cluster, $(N_2)_{13}$, no molecular dissociation, and (almost) no vibrational excitation occur. Hence, the only new energy channel is the rotation energy $E_{\rm rot}$ of the free molecules. We subtract this energy from the internal kinetic energy $E_{\rm int}^{\rm kin}$. Thus the energy balance reads

$$E_0 = E_{\rm trans} + E_{\rm int}^{\rm kin} + E_{\rm int}^{\rm pot} + E_{\rm rot}; \qquad (9)$$

2. for the *weakly-bound molecular* cluster, $(\psi_2)_{13}$, vibrational excitation and molecular dissociation may occur. For a number $N_{\rm mol}$ of surviving free molecules, we count a vibrational energy

$$E_{\rm vib} = \sum_{j=1}^{N_{\rm mol}} \left[\frac{\mu}{2}(v_j^{\parallel})^2 + E_{\rm intra}^{\rm pot}\right], \qquad (10)$$

where $v_j^{\parallel}$ is the projection of the relative velocity of the two atomic constituents of molecule j on the bond axis, μ is the reduced mass and $E_{\rm intra}^{\rm pot}$ is the intramolecular potential excitation energy in the potential, equation (1). The dissociation energy is simply given as

$$E_{\rm diss} = (13 - N_{\rm mol})D. \qquad (11)$$

Thus we have the following energy balance

$$E_0 = E_{\rm trans} + E_{\rm int}^{\rm kin} + E_{\rm int}^{\rm pot} + E_{\rm intra}^{\rm pot} + E_{\rm rot} + E_{\rm vib} + E_{\rm diss}. \qquad (12)$$

The three energy terms $E_{\rm int}^{\rm kin}$, $E_{\rm int}^{\rm pot}$, and $E_{\rm intra}^{\rm pot}$ measure the internal energy of *clusters* while $E_{\rm rot}$ and $E_{\rm vib}$ denote the internal energy of *free* molecules.

Figure 5 shows these contributions for the case of the N_2 cluster. Here, virtually no vibrational excitation occurs; the largest value is measured at $E_0 = 20$ eV and amounts to $E_{\rm vib} = 2$ meV, corresponding to a fraction of 10^{-4} of the impact energy, E_0. The partitioning between internal excitation and fragmentation is similar to the case of the atomic cluster. At energies of E_0 between 1 eV and 6 eV, a considerable amount of intermolecular excitation energy, $E_{\rm int}^{\rm kin}$, is found in the fragments; this is in contrast to the case of the atomic cluster. However, with increasing bombarding energy, the contribution of the rotational energy becomes increasingly larger. Note that at the highest impact energies considered, the cluster has fragmented mainly to individual monomers. Figure 5c shows the rotational excitation of isolated molecules relative to their translational energies. It shows an interesting behaviour. The first free molecules are generated at $E_0 = 0.3$ eV. Up to an energy of $E_0 = 1$ eV, these molecules have been generated in the partial fragmentation regime, in which the major fraction of the impact energy is transformed into 'temperature', i.e., internal kinetic and potential energy

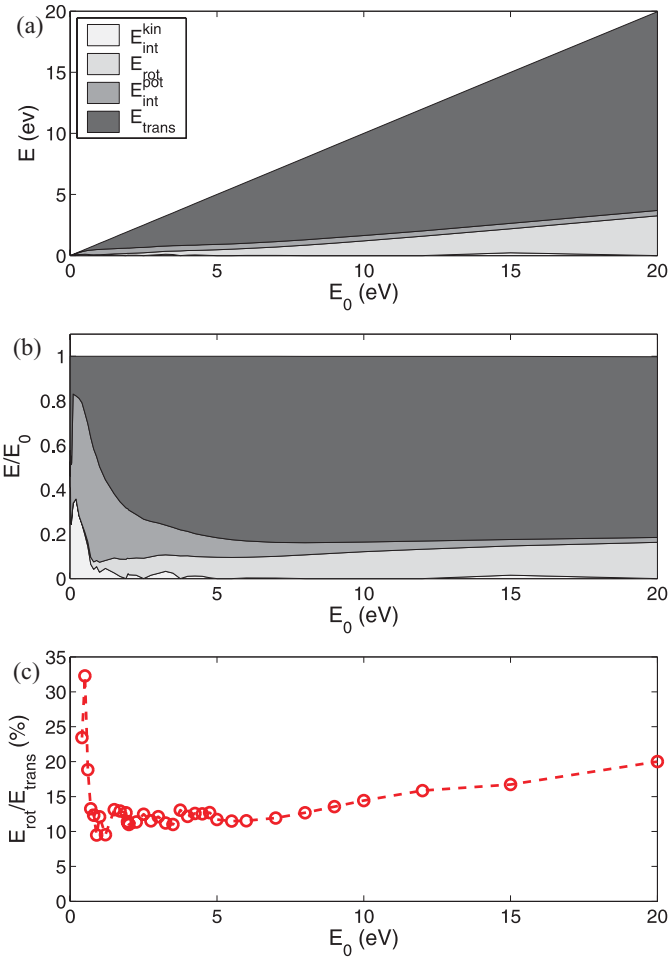

Fig. 5. (a) and (b) Analogous for $(N_2)_{13}$. (c) Ratio of rotational energy of isolated monomers to their translational energy.

and hence also rotational excitation. Above 1 eV, the major fraction of the impact energy goes into translational motion of the fragments. At this point the rotational energy of molecules amounts only to around 10−15% of the translational energy. This fraction steadily increases with impact energy and reaches around 20% at $E_0 = 20$ eV. This ratio is far away from that holding in thermodynamic equilibrium which is governed by the activated degrees of freedom and would be 2/3; this gives evidence of the strongly non-equilibrium nature of the monomer formation process.

Figure 6 shows the most complex case, the soft cluster $(\psi_2)_{13}$. Here, in addition to all the energy channels discussed above, also vibrational excitation of the ψ_2 molecules and their dissociation are found. Vibrational excitation starts at around $E_0 = 1$ eV, somewhat later than when also rotational excitation begins. Both reach maximum values at around $E_0 = 3$−4 eV; for larger impact energies, these contributions become smaller due to the increasing dissociation of molecules.

Figure 6c shows the energy partitioning in the isolated monomers created after impact. The rotational energy

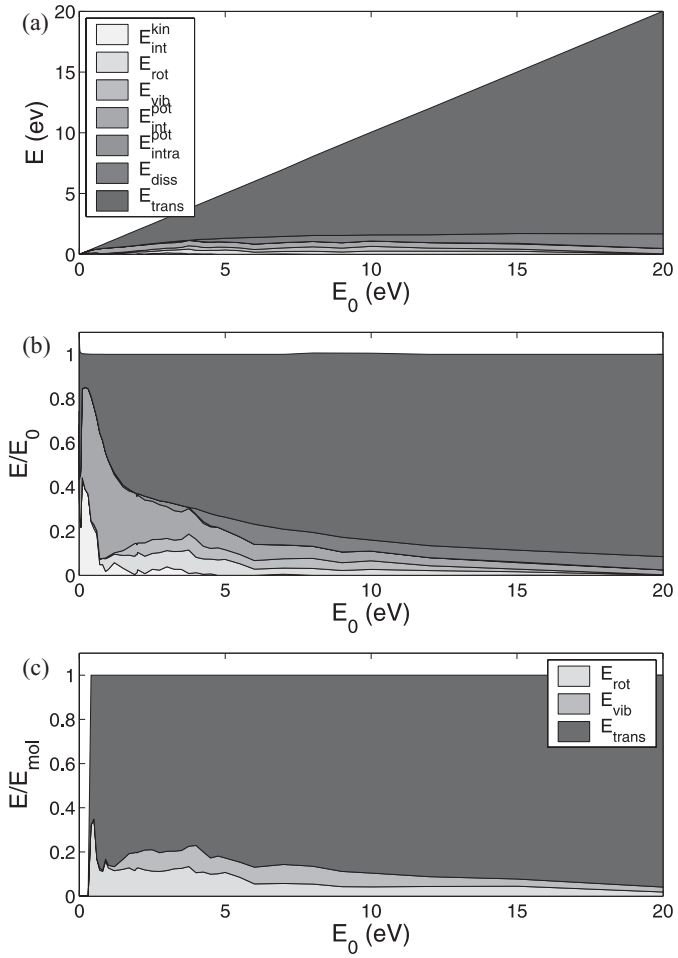

Fig. 6. (a) and (b) Analogous for $(\psi_2)_{13}$. (c) Partitioning of the energy, E_{mol}, of isolated ψ_2 monomers into their rotational, vibrational, and translational contributions.

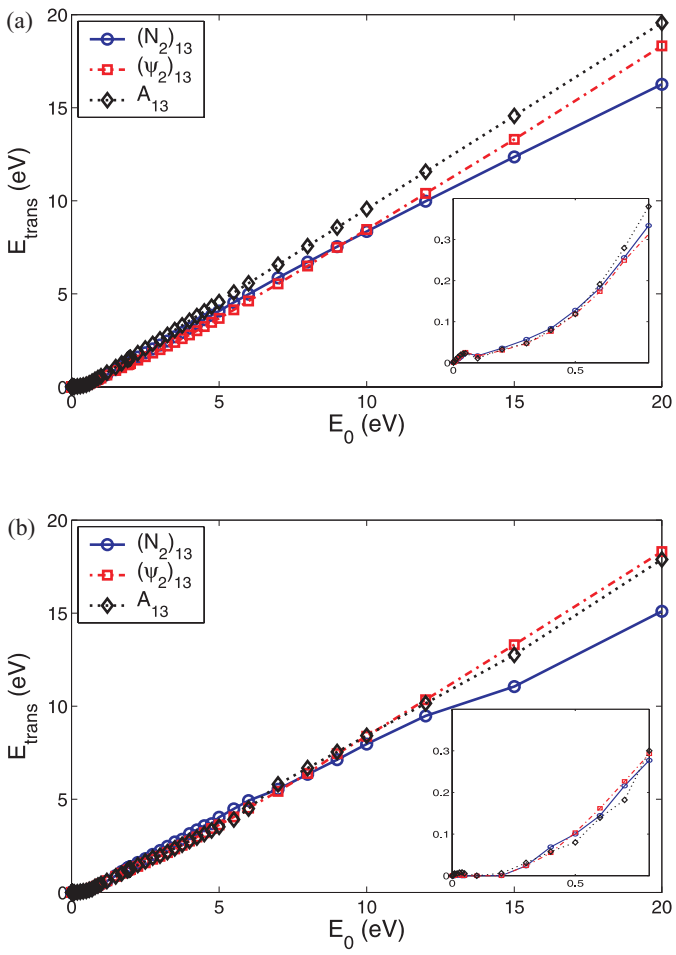

Fig. 7. (Color online) Comparison of translational energies E_{trans} of clusters vs. impact energy E_0 after reflection from a repulsive wall (a) and an attractive wall (b).

behaves similar as in the case of the N_2 cluster, Figure 5c. However, rotational and vibrational excitation attain similar values. This equilibrium reached gives evidence of a statistical population of the internal molecular degrees of freedom, in which the two rotational degrees of freedom attain the same energy as the vibrational degree of freedom. From our consideration of the molecule excitations shown in Figures 5c and 6c, we hence conclude that the molecular translation is not in equilibrium with the internal degrees of freedom, while rotation and vibration are in equilibrium. This can be understood from a molecule formation process in the hot, dense collision zone at the surface, where enough collisions occur to establish an equilibrium of the internal degrees of freedom, while the translation is mainly dictated by the impulsive reflection of the cluster off the surface, and hence does not participate in the equilibrium. Thus our findings show that the concept of a *temperature*, implying thermal equilibration among the atoms or molecules, and in particular between their different degrees of freedom, must be used with care. This applies in particular to the concept of *thermal femtosecond chemistry*, as introduced by Schek et al. [20], but also to statistical approaches such as that by Raz et al. [18], who employ concepts such as the *temperature after impact*.

Thus we conclude that besides the obvious possibilities for intramolecular excitation, the energy redistribution follows quite generally the trend seen for atomic clusters. An immediate consequence of the opening of intramolecular energy channels is, however, that less energy is fed into the translational energies. Since these are most easily measured in time-of-flight experiments, this effect will now be discussed in more detail.

For this purpose, Figure 7 compares the translational energies for the three cases. Due to the occurrence of further energy loss channels, the translational energy of the molecular clusters is (for $E_0 > 2$ eV) always smaller than that of the atomic cluster. However, the translational energies of the N_2 and ψ_2 clusters show an interesting dependence on the impact energy E_0: (i) For $E_0 < 9$ eV, the ψ_2 system shows the smallest translational energy. This can be understood, since for ψ_2, both rotation and vibration can be excited, and hence the center-of-mass translational energy of the reflected fragments is decreased, while in N_2 no vibration can be excited. (ii) For $E_0 > 9$ eV, N_2 has the smallest translational energy. At these impact

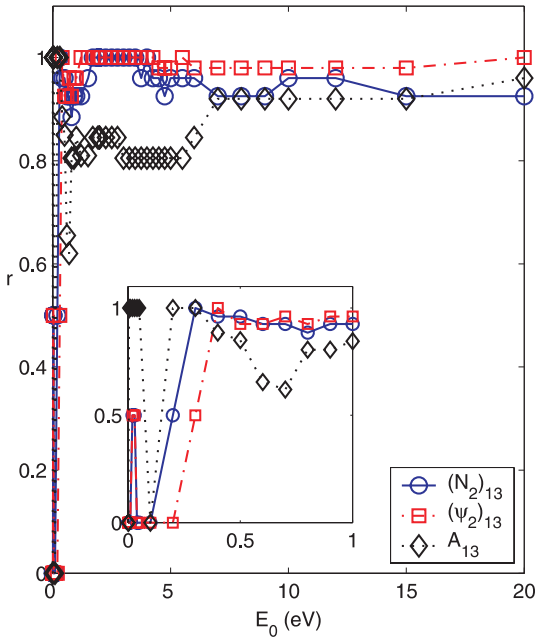

Fig. 8. (Color online) Particle reflection coefficient r after reflection of the cluster from an attractive wall.

energies, more and more ψ_2 molecules will be dissociated so that no energy channels for internal excitation of the molecules remain and hence the total impact energy — besides the fragmentation and dissociation energy — is fed into center-of-mass motion. For N_2, however, due to the strong intramolecular bonding, a considerable fraction of the impact energy goes into molecular rotation, cf. Figure 5c.

4 Results: reflection from an attractive wall

4.1 Sticking

At an attractive wall, particles may be adsorbed, while for the purely repulsive wall studied above, always all cluster fragments are reflected. Thus, even for the extremely small attraction, $\epsilon_w = 3$ meV, sticking of the entire cluster or of some of its fragments to the wall may occur as a new feature. Hence here the reflection coefficient r, which is the number of reflected monomers divided by the number initially in the cluster, 13, is of prime interest. The data on the coefficients are assembled in Figure 8, which shows a complex behaviour. At very small impact energies, $E_0 < 0.3$ eV, the atomic cluster is almost always reflected off the surface, thus reproducing the regime of intact reflection discussed above for a repulsive wall. Here, the passage through the attractive well occurs adiabatically, such that the cluster dynamics is similar to the case of a purely repulsive potential. Note that at these energies, the molecular clusters do not reach 100% reflection; here, the more complex cluster structure allows to transform a larger fraction of the impact energy into internal kinetic energy of the cluster and hence to increase its sticking probability.

A novel regime occurs for energies up to 0.3–0.4 eV for the molecular clusters and at around 0.1 eV for the atomic cluster: Here 'intact sticking' occurs. Here, by the conversion of the impact energy E_0 into internal excitation — which can be performed with 80% efficiency in our cases, see Figures 4–6 — the clusters may lose even more energy after acceleration in the attracting potential well of the wall and thus become bound in it. An inspection of Figure 8 shows that this 'intact sticking' is even more probable for molecular clusters than for the atomic cluster. This is due to the fact that the intramolecular degrees of freedom open up further channels to get rid of the translational energy of the cluster and hence to adsorb it at the surface.

For larger E_0, in the regime of partial fragmentation (0.2–10 eV), it is interesting to note that molecular clusters are totally reflected, while some 20% of the atomic cluster may stick to the wall. This becomes again understandable from the intramolecular degrees of freedom of the molecular clusters, which are strongly excited in the collision process; their energy can be used to liberate cluster fragments from the attractive wall — note that its attraction well is only 3 meV.

Another interesting feature is the difference of the reflection coefficients of the N_2 and the ψ_2 cluster. For large projectile energies, we note that the ψ_2 cluster almost completely dissociates, cf. Figure 2f. Figure 8 now proves that one or two of these atoms remain bound to the attractive wall for energies $E_0 > 5$ eV. In the case of the N_2 cluster, however, always complete N_2 molecules stick and no dissociation occurs.

We note that reflection coefficients $r < 1$ may denote that (i) the cluster fragmented and some fragments stick to the wall, while others are reflected; (ii) dissociated atoms stick to the wall (in the case of ψ_2 only), (iii) a strong dependence on the cluster orientation occurs; thus, for instance, in the regime of intact reflection, at very small energies, the cluster remained intact, and was — depending on the orientation — either reflected or adsorbed intact. Figure 8 displays the average of the two geometries studied. We note that we found this strong orientation dependence only for the reflection coefficient of molecular clusters, but not in the analysis of any other quantity studied in this paper, and not for atomic clusters.

In conclusion, we see that even a very faint attractive wall — like the one studied here $\epsilon_w = 3$ meV — exerts a major influence on the reflection behavior of clusters impacting on a surface. Total sticking of a cluster becomes possible for low bombarding energies, in the regime where a repulsive wall shows intact reflection. A distinct difference between atomic and molecular clusters becomes evident in that the intramolecular degrees of freedom can (i) act as an energy *sink* to bind slow molecules even stronger to the wall, and (ii) as an energy *source* to liberate small cluster fragments, and in particular molecular monomers, from the wall at higher impact energies. Even the effect of dissociative bonding is observable in our simple model.

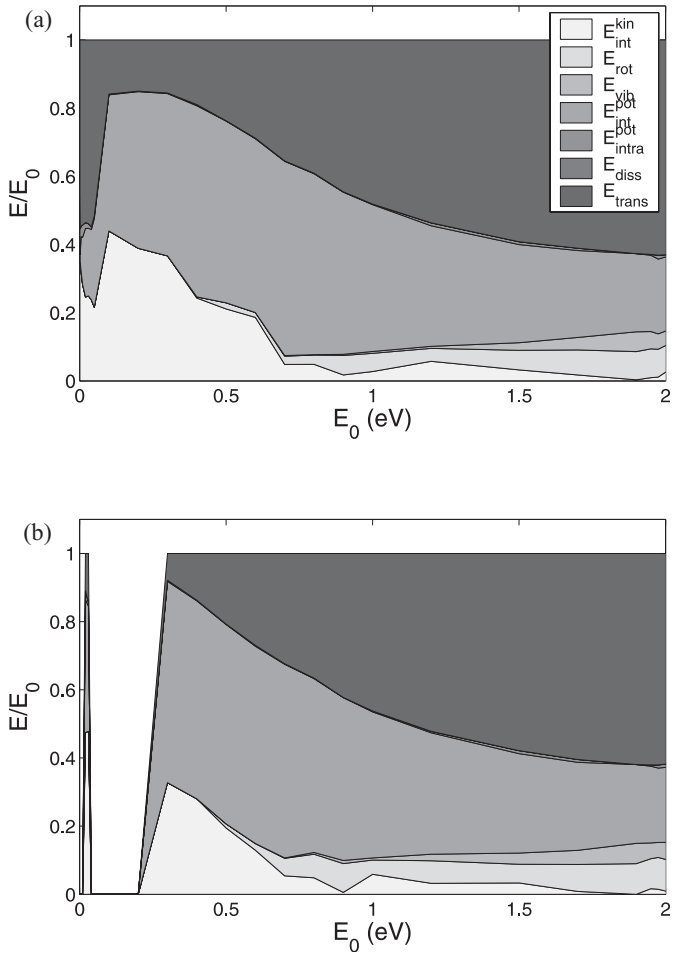

Fig. 9. Energy redistribution of ψ_2 clusters after reflection from (a) a repulsive and (b) an attractive wall. Only clusters impinging in the tip geometry have been considered.

4.2 Energy redistribution

The analysis of energy redistribution in the presence of an attractive wall is not so straightforward due to 2 effects: (i) in experiment, only reflected particles are measured and accordingly we shall only be interested in their properties; thus, the energy of the adsorbed particles is missing from our balance — this complicates in particular the analysis of the intermolecular potential energy. (ii) If part of the cluster is trapped in the attractive well of the wall, the remainder of the reflected cluster will gain energy. Hence we plot in Figure 9 only the energy contributions of reflected particles. Furthermore, we restrict our analysis to clusters impinging on the surface in the tip geometry. In this case we found that either the entire cluster sticks to the wall or is reflected; thus the restriction to this case simplifies our analysis. Since, as noted above, the fragmentation patterns and energy redistribution channels for the two geometries studied (tip and face geometry) differed only marginally, we are confident that our energy analysis performed here for the tip geometry will give satisfactory results.

We found the energy distributions of the reflected particles to be quite similar to those for a repulsive wall. Differences occur mainly at very low bombarding energies, in the regime where the repulsive wall reflects the cluster intact, while the attractive wall can bind the entire cluster to it. As an example for the different energy redistributions, Figure 9 compares the energy redistribution for the ψ_2 cluster scattered off a repulsive wall with that scattered from an attractive wall. At very small impact energies ($E_0 = 20{-}30$ meV), the cluster is reflected intact. Reflection off an attractive wall leads to a higher internal excitation, as measured by $E_{\rm int}^{\rm kin}$ and $E_{\rm int}^{\rm pot}$. As a consequence, only around 15% of the impact energy is used for center-of-mass motion of the reflected cluster off the wall; this has to be compared with the reflection off a repulsive wall, where 55% of E_0 is used for translational motion. For higher impact energies, cluster excitation becomes stronger ($E_0 = 0.2{-}0.3$ eV). In this case the collision with an attractive wall leads to such a high internal excitation, that the cluster remains bound to the surface, and the reflection coefficient is zero. When cluster reflection sets in, at $E_0 \geq 0.3$ eV the energy redistribution in the scattered cluster and its fragments is only very weakly influenced by the presence of the attractive wall. We note that at high energies E_0, the reflected energies are quite analogous to those for a repulsive wall.

Finally, in Figure 7b, we display the translational energies of reflected clusters, and compare to those reflected from a repulsive surface, Figure 7a. Here again the average over the tip and the face geometry is shown. Evidently, the existence of a tiny attraction well such as the one chosen here, $\epsilon_w = 3$ meV, has a major influence on the translational energies of reflected particles, even at the highest impact energies simulated, $E_0 = 20$ eV. Note first that the ordering, in which reflected clusters assume the highest translational energy for given E_0, differs strongly from the results of a repulsive wall. Second, the translational energies are distinctly smaller than for a purely repulsive wall; at $E_0 = 20$ eV, this effect may amount up to 2 eV! The reason for this strong influence lies in the fact that the reflection coefficient $r < 1$ for energies up to the highest energies simulated, $E_0 = 20$ eV. For instance, in the case of $(N_2)_{13}$, a single N_2 molecule remains bound with rather high rotation energy in the attractive well, thus reducing the total measured translational energy. Note that in the case of the ψ_2 cluster, where the reflection coefficient is almost 1 throughout the range of impact energies studied, the translational energy curves with and without attractive well coincide rather well.

5 Conclusions

Using molecular-dynamics simulation, we studied the processes occurring after impact of clusters containing 13 atoms or molecules on a rigid wall. Both an atomic cluster and a molecular cluster were investigated; the

intramolecular bond was chosen (at least) an order of magnitude larger than the intermolecular bond.

1. Four different regimes in the fragmentation behavior could be identified. In the order of increasing projectile energy they are: (i) intact reflection of an internally excited cluster — this includes the possibility of 'intact sticking' at an attractive wall; (ii) shattering of the cluster to several large pieces; (iii) complete fragmentation to monomers; (iv) dissociation into atoms.
2. At low impact energies E_0, the majority of the impact energy is converted to internal energy of the cluster, whereas at high E_0, the energy is used for the translational center-of-mass energy of the reflected fragments and the ro-vibrational excitation of molecular monomers.
3. For an attractive wall, the largest sticking coefficient is observed in the low-energy regime of intact reflection [item (i) above], where the entire cluster sticks without fragmenting. In the shattering regime, atomic clusters show a superior sticking as compared to molecular clusters. Even for the weak attractive well studied here, $\epsilon_w = 3$ meV, the reflection coefficient $r < 1$, even for impact energies $E_0 = 20$ eV.
4. The translational center-of-mass energy of reflected fragments depends sensitively on the details of the inter- and intramolecular bonding in the cluster. As a rule, with increasing number of degrees of freedom which can be activated in the collision, the translational energy sinks. Thus, the atomic cluster shows the highest translational energies. On the other hand, for weak intramolecular bonding, intramolecular vibrations are easily excited at small impact energies, reducing the resulting translational energy. At high impact energies the molecular dissociation closes this channel, and the translational energy increases with respect to more strongly-bonded molecules.
5. In particular, the regime of intact reflection is extended to larger bombarding energies for molecular clusters than for atomic clusters; here, the internal degrees of freedom help in stabilizing the clusters.
6. For molecular clusters, we find that rotational and vibrational degrees of freedom of the fragmented cluster are in equilibrium, such that the two rotational degrees of freedom of monomer molecules reach the same energy as the vibrational degree of freedom. However, the major fraction of the impact energy goes into translational motion of the fragments, such that translation does not participate in thermal equilibrium.
7. Even a tiny attractive surface potential has a major influence on the translational energies of reflected particles, even at impact energies that are much higher than the attractive well.

In this work, we concentrated on a systematic comparison of atomic vs. molecular clusters colliding with a solid rigid wall at hyperthermal energy. For this purpose, a (spherical) Lennard-Jones cluster of fixed size (13 monomers) was chosen. Several routes for extending this study appear interesting: (i) collision of an *ionized* cluster: this could bring the investigation into closer contact with experiments, where the properties of ionized fragments are measured; (ii) the study of the influence of the *cluster size*; (iii) the influence of an *atomically structured wall* instead of the flat rigid wall used in the present paper; and finally (iv) the effect of a *stronger adsorption well* at the scattering wall.

We gratefully acknowledge discussions with W. Christen, which inspired us to perform this work, and his valuable comments on the manuscript.

References

1. C.L. Cleveland, U. Landman, Science **257**, 355 (1992)
2. B. Gergen, H. Nienhaus, W.H. Weinberg, E.W. McFarland, Science **294**, 2521 (2001)
3. W. Harbich, in *Metal Clusters at Surfaces: Structure, Quantum Properties, Physical Chemistry* (Springer, Berlin, 2000), Springer Series in Cluster Physics, p. 107
4. H.-P. Cheng, U. Landman, Science **260**, 1304 (1993)
5. I. Yamada, J. Matsuo, Z. Insepov, T. Aoki, T. Seki, N. Toyoda, Nucl. Instrum. Meth. B **164-165**, 944 (2000)
6. W. Christen, U. Even, J. Phys. Chem. A **102**, 9420 (1998)
7. F.O. Goodman, H.Y. Wachman, *Dynamics of gas-surface scattering* (Academic Press, New York, 1976)
8. C.T. Rettner, M.N.R. Ashfold, *Dynamics of gas-surface interactions* (Royal Society of Chemistry, Cambridge, 1991)
9. R.M. Logan, R.E. Stickney, J. Chem. Phys. **44**, 195 (1966)
10. R.M. Logan, J.C. Keck, J. Chem. Phys. **49**, 860 (1968)
11. H. Gades, H.M. Urbassek, Appl. Phys. A **61**, 39 (1995)
12. A. Tomsic, P.U. Andersson, N. Markovic, J.B.C. Pettersson, J. Chem. Phys. **119**, 4916 (2003)
13. A. Tomsic, H. Schröder, K.-L. Kompa, C.R. Gebhardt, J. Chem. Phys. **119**, 6314 (2003)
14. W. Christen, U. Even, T. Raz, R.D. Levine, J. Chem. Phys. **108**, 10262 (1998)
15. G.-Q. Xu, S.L. Bernasek, J.C. Tully, J. Chem. Phys. **88**, 3376 (1988)
16. J.N. Beauregard, H.R. Mayne, J. Chem. Phys. **99**, 6667 (1993)
17. E. Hendell, U. Even, T. Raz, R.D. Levine, Phys. Rev. Lett. **75**, 2670 (1995)
18. T. Raz, U. Even, R.D. Levine, J. Chem. Phys. **103**, 5394 (1995)
19. W. Christen, U. Even, T. Raz, R.D. Levine, Int. J. Mass Spectrom. Ion Proc. **174**, 35 (1998)
20. I. Schek, T. Raz, R.D. Levine, J. Jortner, J. Chem. Phys. **101**, 8596 (1994)
21. W. Christen, U. Even, Eur. Phys. J. D **9**, 29 (1999)
22. T. Raz, R.D. Levine, J. Chem. Phys. **105**, 8097 (1996)
23. G. Herzberg, *Molecular Spectra and Molecular Structure*, (van Nostrand, Toronto, 1950), Vol. 1
24. A. Lofthus, P.H. Krupenie, J. Phys. Chem. Ref. Data **6**, 113 (1977)
25. T.A. Scott, Phys. Rep. **27**, 69 (1976)
26. C.S. Murthy, K. Singer, M.I. Klein, I.R. McDonald, Molec. Phys. **41**, 1387 (1980)
27. M.R. Hoare, P. Pal, Adv. Phys. **20**, 161 (1971)
28. H. Gades, H.M. Urbassek, Phys. Rev. B **51**, 14559 (1995)
29. S.D. Stoddard, J. Comput. Phys. **27**, 291 (1978)
30. R.D. Levine, R.B. Bernstein, *Molecular reaction dynamics and chemical reactivity* (Oxford University Press, Osford, 1987)